CSIRO
AUSTRALIA

The CSIRO 9-level Atmospheric General Circulation Model

J.L. McGregor, H.B. Gordon, I.G. Watterson,
M.R. Dix and L.D. Rotstayn

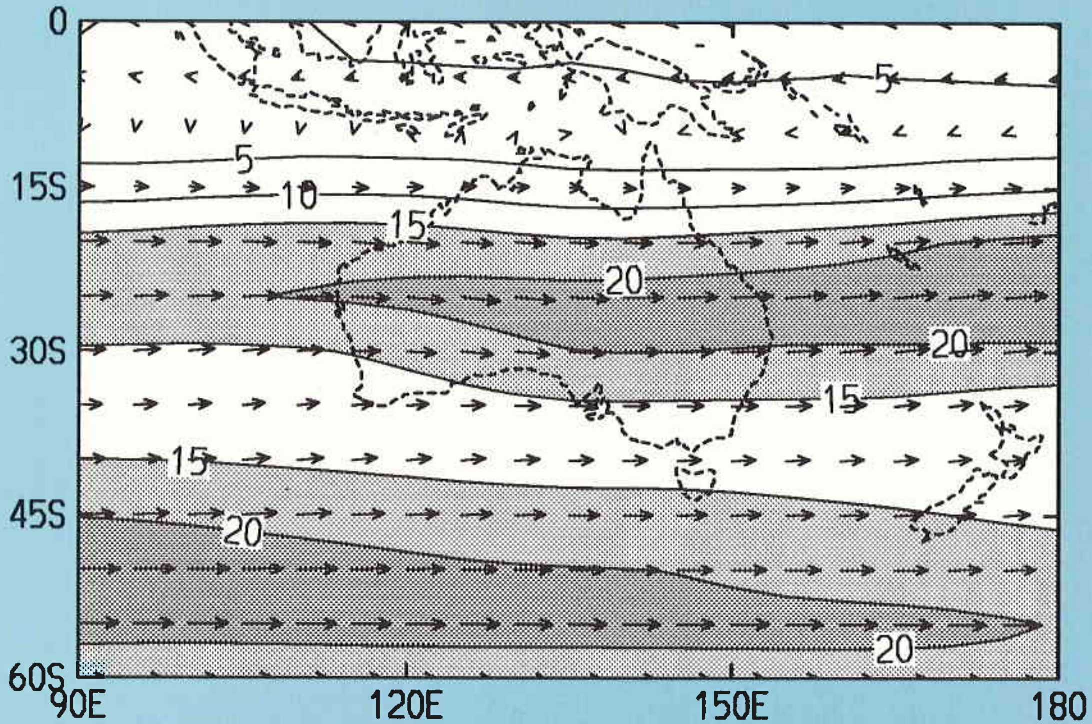

CSIRO9 500 hPa winds (JJA, m s^{-1})

CSIRO DIVISION OF ATMOSPHERIC RESEARCH TECHNICAL PAPER No. 26

The CSIRO 9-level Atmospheric General Circulation Model

J.L. McGregor, H.B. Gordon, I.G. Watterson,
M.R. Dix and L.D. Rotstayn

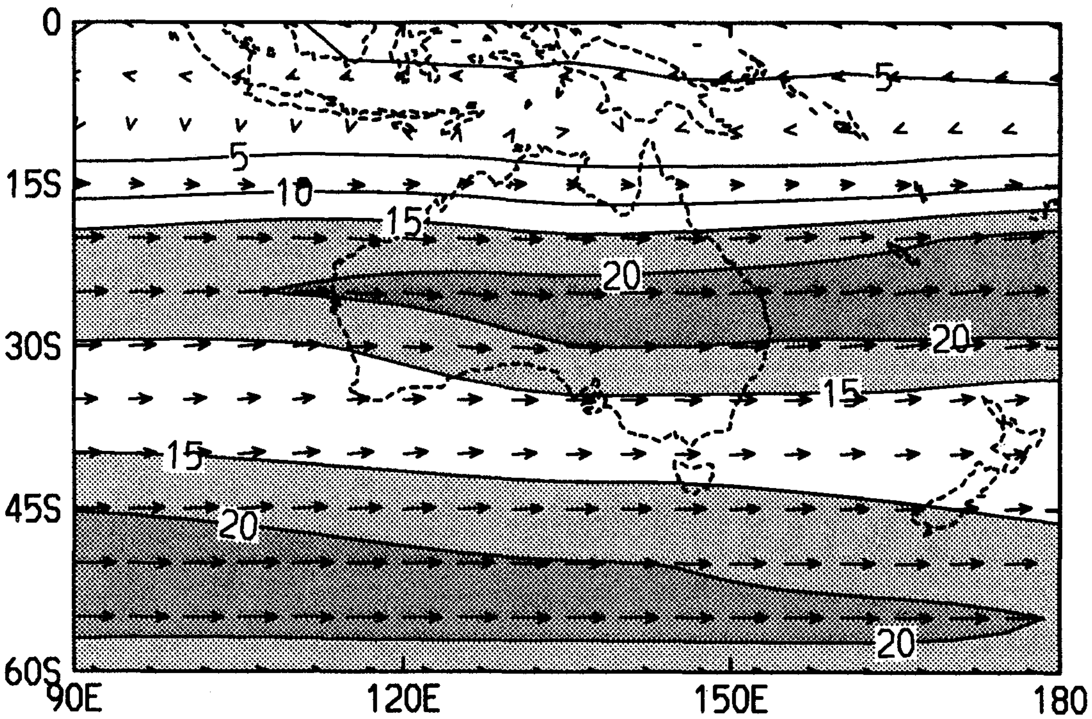

CSIRO9 500 hPa winds (JJA, m s^{-1})

CSIRO DIVISION OF ATMOSPHERIC RESEARCH TECHNICAL PAPER No. 26

National Library of Australia Cataloguing-in-Publication Entry

The CSIRO 9-level atmospheric general circulation model

Bibliography ISBN 0 643 05250 X

1. Atmospheric circulation - Mathematical models.
I. McGregor, J.L. II. CSIRO Division of Atmospheric Research.
(Series: CSIRO Division of Atmospheric Research Technical Paper; no. 26).

551.517

Front cover: Mean 500 hPa winds for June-August as simulated by the CSIRO9 model, showing the split jet. The arrows show the wind direction. The contours show the magnitude of the wind, with light shading used for 15-20 m s^{-1} and dark shading above 20 m s^{-1}.

© CSIRO Australia 1993

Printed on recycled and environmentally friendly paper

Contents

		Page
1	Introduction	1
2	Model structure	2
3	Interface to the physical processes	7
4	Surface characteristics	8
5	Surface fluxes	11
6	Soil and surface temperatures	13
7	Soil moisture	15
8	Time integration of surface properties	16
9	Vertical mixing and shallow convection	18
10	Gravity wave drag	21
11	Radiation parameterization	24
12	Cloud prediction	27
13	Rainfall and cumulus convection	29
14	Frictional heating	30
15	Non-linear dynamics and energy conservation	31
16	Time integration and temporal smoothing	33
17	Horizontal diffusion	34
18	Model climatology	36
	Acknowledgements	41
	References	41
	Appendix A: List of symbols and abbreviations	44
	Appendix B: Screen temperatures	46
	Appendix C: Cumulus convection details	48
	Appendix D: Particle trajectory facility	53
	Appendix E: List of subroutines	54
	Appendix F: Figures of model climatology	55

1. Introduction

Numerical models of the general circulation of the atmosphere are an important tool in climate research. They have been used to investigate the dynamical and physical processes controlling the atmosphere. The incorporation of representations of the cryosphere and oceans into such a model allows it to be used for forecasting climate anomalies and climate change. The spectral 9-level Atmospheric General Circulation Model (AGCM) described in this report has been developed at the CSIRO Division of Atmospheric Research to provide the basis for the current greenhouse research project and for future research.

The spectral method for modelling the general circulation of the atmosphere is now firmly established (Bourke 1974; McAvaney et al. 1978) and has been adopted at several major research centres including the National Center for Atmospheric Research (NCAR), the European Centre for Medium-range Weather Forecasting (ECMWF), and the Canadian Climate Centre. It provides a cost effective means of atmospheric modelling which is essential for climate research.

The original CSIRO spectral AGCM had 2 vertical levels, and was developed at the Australian Numerical Meteorology Research Centre (Gordon 1983; Gordon and Hunt 1987; Hunt and Gordon 1988, 1989). From this model a 4-vertical-level model (CSIRO4) was developed at the CSIRO Division of Atmospheric Research (Gordon and Hunt 1991; Hunt and Gordon 1991; Smith and Gordon 1992), as documented by Gordon (1993). The present 9-level model (hereafter referred to as CSIRO9) was subsequently developed from this model.

The version of the CSIRO9 model described here has been used to generate the implied ocean heat transports required to enable computation of sea temperatures by a slab ocean model rather than using prescribed temperatures. The inclusion of this simple "mixed-layer" ocean into the model allows the lower boundary condition involving the land surfaces, the polar ice caps, and now the oceans to be self-determining. This form of the CSIRO9 model is currently being used for greenhouse research and will be documented elsewhere.

This publication documents the formulation of CSIRO9 and is intended as a general guide to its contents and formulation. It does not give details of the model's computer coding as would be required by users wishing to modify the model. The description of the dynamical framework of the model has been kept to a minimum since standard spectral techniques have been used. On the other hand, the physical processes are comprehensively covered.

The physical structure of the model (horizontal and vertical resolution) is detailed in the next section, and provides an overview of the formulation used in the computer code. The subsequent sections have been given in a sequence which follows as closely as possible the steps involved in the computer code to complete a timestep. Sections 3 - 14 contain details of the methods used to implement the physical parameterizations in the model. Section 15 gives brief details of considerations used when formulating the non-linear dynamics so that energy conservation is achieved. Section 16 and 17 describe the final time integration of the main prognostic variables, and the application of spectral horizontal diffusion.

The model description is followed by a short section on the model climatology (Section 18). A range of important climatic variables produced by the model over a 10-year run is presented. The observed fields are displayed for comparison wherever possible. The overall climate produced by this version of the model is acceptable by current standards of the international climate modelling community. Areas of the model simulation which might be improved are discussed where appropriate.

A trajectory (tracer) facility has been incorporated into the model, with a view to using the CSIRO9 model to study phenomena such as the emission of debris from volcanoes, and the release of possibly harmful materials into the atmosphere (e.g. during the "Gulf" war). Details are given in Appendix D.

The model has a comprehensive physical and dynamical diagnostics package, with a convenient print out of major fields (some as global maps and some as zonal averages). Data files of monthly averages of the most important global dynamical and physical quantities are created. There is also a facility for storing data over a specific region on a daily basis. Various surface fields for a small number of individual grid-points can also be saved at each timestep.

2. Model structure

The CSIRO9 model performs a forward-in-time integration of the primitive equations describing the motion of the global atmosphere. The model simulates a comprehensive range of "physical" processes including radiation and precipitation which act as forcings of the dynamical equations. The model is intended for general climate simulation and thus represents full annual and diurnal cycles. The lower boundary condition for the atmosphere is determined by an interactive land surface scheme but sea-surface temperatures are prescribed in the model version described here. All other major properties such as cloud amount, snow, and sea-ice are self-determining.

The model utilizes the "flux" form of the dynamical equations (Gordon 1981) rather than the "advective" form (see for example, Bourke 1974). The flux formulation ensures that conservation of mass and energy can be readily achieved (unlike the advective formulation). This conservation is vital for an AGCM which is to be used for the multi-annual integrations required for climate investigation. Details of the derivation of the model dynamical equations are given by Gordon (1981, 1993).

Horizontal and vertical resolution

The vertical structure of the model is given in Figure 1. Standard notation is used for variables wherever possible, and a listing of all variables is given in Appendix A. The model utilizes the sigma ($\sigma = p/p_s$) coordinate in the vertical. The vertical level spacing need not be uniform. The main prognostic variables of the model are the surface pressure p_s, and the surface pressure weighted divergence ($\hat{D}$), vorticity ($\hat{\zeta}$), temperature ($\hat{T}$), and moisture ($\hat{q}$). The divergence and vorticity have an associated velocity potential ($\hat{\chi}$) and stream function ($\hat{\psi}$). The variables are carried as spectral (complex or split real/imaginary) fields except for moisture which is a grid variable. The main prognostic variables are carried at full-levels, whilst the diagnostics of "vertical" velocity ($\dot{\sigma}$) and geopotential height are essentially derived at half-levels; the full-levels are located midway between the half-levels.

The model has been coded for variable spectral (horizontal) resolution, and the most appropriate resolutions are usually based upon the number of east-west grid-points being some power of 2. This enables an efficient usage of currently available Fast Fourier Transform routines (FFTs). The current CSIRO 9-level model is run at a spectral resolution of R21 (rhomboidal truncation at 21 waves) which utilizes an equally spaced east-west grid of 64 and a pole to equator grid of 28 unevenly spaced latitudes per hemisphere. This grid resolution is sufficient to give alias-free evaluation of quadratic terms via the grid transform method of

Bourke (1974). A semi-implicit leapfrog time scheme is used (current and previous timestep values are retained) together with a Robert (Asselin) time filter. The R21 model timestep is 30 minutes.

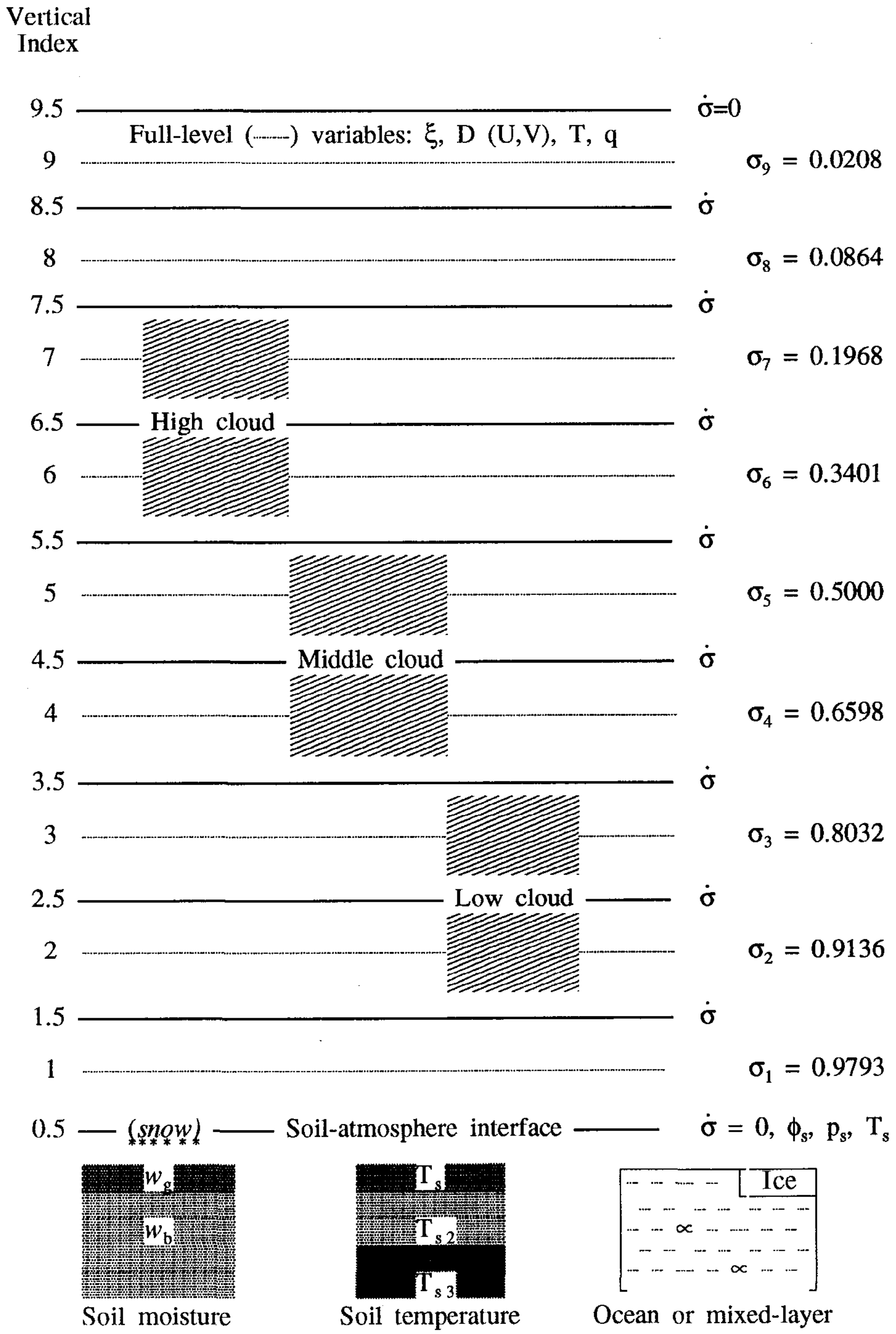

Figure 1. Level structure of the CSIRO9 model. Variables are defined in Appendix A.

Model flow diagram

The sequence of operations during each timestep is illustrated in Figure 2, where some subroutine names have been included as a guide for model users. A more complete list of subroutine names is given in Appendix E. The model has been coded for use with a coupled ocean model, but in this document only the atmospheric component is discussed. The atmospheric part of the combined model is controlled by the routine *CSIRO9*. This routine controls the initialization of the model (the main model constants are set in *inital* and *initax*, the two restart files are read via *filerd*, and the Gaussian latitudes and Legendre polynomials are created in *gauleg*). There then follows a sequence of subroutine calls which takes the model through repeated timesteps - the Timestep loop.

The major components involved in each timestep are as follows. From the spectral input data for the stream function and velocity potential, the spectral fields for U and V are obtained (*uvharm*). At the same time, the spectral equivalents for $\partial U_{fr}/\partial t$, $\partial V_{fr}/\partial t$ (which are the frictional dissipation terms from the previous timestep) are also created. These will be used to determine the frictional heating of the atmosphere. This particular part of the model physics is discussed more fully in Section 14.

The model then enters the Physics transform loop. Noting that the main prognostic variables of the model ($\hat{\chi}$, $\hat{\psi}$, $\hat{T}$, p_s, $\hat{q}$) have just been updated via the previous time integration (or the equivalent fields read from the restart file), the temperature and moisture fields in particular then need to be adjusted for the physical parameterizations of rainfall, convection and vertical mixing. There will also be implied adjustments to the momentum fields via surface drag, turbulent mixing and gravity wave drag. All of the physical parameterizations (see Sections 3 - 14) are achieved during the Physics loop which transforms spectral data to equivalent grid-point fields in order to perform these adjustments. More details of the methodology used in the Physics transform loop, and a subsequent Dynamics transform loop are given in the next sub-section entitled *Grid transforms*.

The next part of the timestep evaluates the non-linear part of the tendencies for the $\hat{\chi}$, $\hat{\psi}$, $\hat{T}$ and $\hat{q}$ fields. This is achieved in the Dynamics loop which, like the Physics loop, takes spectral fields and creates grid-point equivalents. The grid-point values are used to determine multiple products on the grid, and by an inverse transform, the relevant spectral tendencies are evaluated. This is the standard spectral technique for such evaluations.

Following the Physics and Dynamics transform loops (Figure 2), the linear part of the spectral tendency equations are added to the non-linear components derived during the Dynamics loop (subroutine *linear*). These linear terms affect the vorticity and divergence equations only. In order to prevent decoupling of the time integrated solution at odd and even timesteps, a Robert time filter is used (see Section 16). This filter is applied in two parts - the first stage being during the time integration (*semii*) and a subsequent part is applied following the physical adjustments (in *assel* on the flow diagram), but before the next timestep.

The time integration of the main atmospheric prognostic variables is then performed (*semii*). The grid-point moisture field is integrated in a simple leapfrog manner. The same method is applied to the spectral vorticity equation (or the stream function equivalent). In the case of the spectral divergence, temperature, and surface pressure equations, a semi-implicit time integration method is used in order to handle gravity waves; see Gordon (1981, 1993) for details. Following the time integration, the spectral horizontal diffusion for the temperature, vorticity and divergence fields are applied in a forward implicit manner for numerical stability (see Section 17). This completes a model timestep.

Initialize model (*inital, initax, filerd, gauleg*)

Timestep loop

Form spectral U_l^m, V_l^m and frictional components (*uvharm*)

Physics loop over latitude pairs, poles to equator (*phys*)

Convert relevant fields from spectral to grid form (*ptog*):

$$\hat{U},\ \hat{V},\ p_s,\ \hat{T},\ \frac{\partial U_{fr}}{\partial t},\ \frac{\partial V_{fr}}{\partial t}$$

Store $\hat{U}$, $\hat{V}$, p_s for use in Dynamics loop
Compute physical parameterizations per latitude
(*radin* which calls *surfset, hsflux, radfs, surfupa, hvertmx, gwdrag, rainda, conv, cvmix, surfupb*)
Update the grid moisture field $\hat{q}$ following evaporation and rain
Reform the spectral temperature $\hat{T}$
Create spectral components for horizontal moisture flux $\nabla.(\underline{V}\ \hat{q})$, and apply moisture diffusion on pressure surfaces ($\nabla^2 p_s$, $\nabla^2 q$)

End of **Physics loop**

Dynamics loop over latitude pairs, poles to equator (*dynm*)

Convert requisite fields from spectral to grid form (*dtog*):

$$\hat{D},\ \hat{\xi},\ \hat{T},\ \nabla p_s,\ \nabla.(\underline{V}\ \hat{q}),\ \nabla^2 p_s,\ \nabla^2 q$$

Compute non-linear flux terms on the grid (*dynmnl*)
Store pressure level data every 6 h (*dynmst*)
Create spectral components of the non-linear parts of the tendency equations

End of **Dynamics loop**

Add the linear spectral tendencies (*linear*)
Apply the Robert (Asselin) time filter (*assel*)
Perform the semi-implicit time integration (*matset, semii*)
Incorporate the forward implicit horizontal diffusion (*diffn*)

End of **Timestep loop**

Print/save statistics (*filest*). Update restart file (*filewr*)

Figure 2. CSIRO9 model flow diagram. A few key subroutine names are given in italics.

Grid transforms

For each timestep, the CSIRO9 model uses two grid transforms. The first is termed the Physics transform loop during which various physical parameterizations are implemented. A second grid transform termed the Dynamics loop follows, in which the non-linear dynamical tendencies are evaluated.

The temperature field will be used as an example to demonstrate the method used in the two grid transforms. During the Physics loop, the temperature is transformed from spectral space (following time integration) into its gridded form. This is achieved in a sequential manner - first the northern-most latitude, then the southern-most latitude, and so on up to the adjacent equatorial latitudes. The temperature field is modified by the physical processes (e.g. rainfall, convection, vertical mixing), and the new spectral field is generated by an inverse transform technique. This new field is then exactly fitted to the spectral resolution of the model.

The updated form of the temperature field is now in a form suitable for application of the horizontal flux calculations (the Dynamics transform) for evaluation of the non-linear part of the temperature tendencies. This again involves a full spectral-to-grid, and subsequent grid-to-spectral transform as in the Physics loop. The use of two transform loops ensures that a spectrally-fitted temperature field is used during the calculation of advective tendencies on the grid. There is only a small computational overhead associated with the second transform loop for temperature.

The transform from complex spectral space to values on the grid is performed by an algorithm which is efficient on vector processing machines. The complex fields are first split into separate real and imaginary components. The Fourier coefficients for a northern hemisphere (NH) latitude and equivalent southern hemisphere (SH) latitude can be obtained at the same time by summing separately the odd and even components (for both real and imaginary parts) for the Legendre part of the transform. This is due to the fact that

$$P_l^m\{\sin(-\phi)\} = (-1)^{l+m}\, P_l^m\{\sin(\phi)\} \tag{2.1}$$

where $P_l^m\{\sin(\phi)\}$ is an associated Legendre polynomial of the first kind normalized to unity. The resultant odd and even sums can be either added or subtracted to give Fourier components for the NH or SH. The FFT routines then generate grid values at the latitude.

The inverse transform, whereby a spectral field is resynthesized from the data on the grid at every latitude, is essentially the reverse of the above. The same efficient odd/even, real/imaginary method is used. A substantial increase in efficiency on vector machines is achieved by using rotated indices for these fields. To clarify this, note that the spectral arrays are normally held as (l, m, k) where l, m denote the Legendre components and k is the vertical level. This is efficient for the spectral-to-grid transform where summation is first carried out over the odd/even l components (a partial cascade sum method is used here). But for the inverse transform, the grid data after using the FFT has Fourier components in the array form (m, k). So for vector efficiency reasons, the spectral resynthesis which involves the sequential addition from contributions at all latitudes is done using temporary arrays of the form (m, k, l), noting that the odd/even technique is now carried out over the *last* index.

In the outline of the grid transforms above, it should be noted that the model has been coded in Fortran specifically for high speed on a vector computer such as a Cray. The current version of the code would thus be inefficient on a scalar machine. The coding also uses calls to specific Cray FFT routines. These routines perform most efficiently when as many variables as possible are transformed (per latitude row) at the same time. For use on other machines, these calls would have to be modified accordingly.

Moisture considerations

Whilst the main dynamical fields of vorticity, divergence, and temperature are carried as spectral fields, the moisture is held as a grid-point field. This is done since moisture is such a highly variable quantity in the horizontal, it suffers unduly from spectral fitting problems. Such problems are especially apparent in the polar regions where spectral fitting can cause some locations to have excessive rainfall.

While the gridded form of the moisture field is ideal for the calculation of physical processes, the horizontal transport of moisture needs special treatment. It is evaluated by a pseudo-spectral technique, whereby the horizontal moisture flux divergence term $\underline{\nabla}.(p_s\underline{V}q)$ is spectrally determined by synthesis during the Physics loop (a standard spectral procedure is used for such divergence evaluations; see e.g. Bourke 1974). The equivalent grid-point values of this tendency are then computed during the subsequent Dynamics loop.

In modelling the transport of a field with large gradients, whether by spectral methods or by grid-point methods, negative values may develop even though the field should be positive-definite. Atmospheric moisture is a difficult variable to model accurately since it has both a large vertical gradient and a large pole to equator gradient. The parameterization of sub-grid-scale horizontal mixing, as described in Section 17, helps to smooth the horizontal structure of the moisture field. Similarly, vertical mixing of moisture (Section 9) also assists. However, there are occasions when the divergence of the moisture field is such that a negative value may occur. To counter this, if the moisture value drops below 2×10^{-6} kg(water)/kg(air) by vertical advection, then the vertical transport is inhibited. Also, following the time integration, the global moisture field at each level is checked for the presence of negative values, and these are removed by a proportional adjustment method, whilst maintaining conservation of global mean moisture.

3. Interface to the physical processes (*phys*)

Most of the model computation is carried out during the Physics transform loop (at R21 resolution the largest portion is concerned with radiative transfer calculations). Because of their complexity each major component of the parameterizations is described in a separate section of this report.

For each latitude row certain grid-point values are evaluated from spectral space (subroutine *ptog*). These include $\hat{U}$, $\hat{V}$, p_s and $\hat{T}$. The momentum tendencies due to the horizontal diffusion of momentum are also obtained. The mixing ratio is already available in grid form. The values of $\hat{U}$, $\hat{V}$, p_s are not altered by the Physics loop and are retained in grid form for the Dynamics loop.

An important physical parameterization calculates the turbulent vertical mixing of momentum, which includes the effect of surface stresses. Special consideration is required in a spectral model, because the implied changes to the velocities would require the resynthesis of the associated spectral vorticity and divergence fields. To improve computational stability these tendencies must be either calculated implicitly (similar to the procedure the model uses for temperature and moisture), or *backward* in time. By taking the latter course, we can apply the vertical mixing tendencies as a grid-point addition to the non-linear dynamics terms, and avoid this resynthesis. It is necessary that these quantities be saved between timesteps.

4. Surface characteristics (*surfset*)

The distribution of land and non-land R21 model grid-points is shown in Figure 3. The spectral method requires that the surface topography be spectrally fitted to a resolution of R21 for use by the model. This initial topography is derived from a 1° x 1° data set, area averaged to the 64 x 56 Gaussian grid, and then spectrally resynthesized to R21 resolution. A consequence of this procedure is non-zero sea elevation (due to the Gibbs phenomenon). The resultant topography is shown in Figure 4.

There are 4 types of surface. These are referenced by a mask (*imsl*) which has values 1 for Ice, 2 for Mixed-Layer Ocean (MLO), 3 for Sea, and 4 for Land. This is *not* a static mask since the model allows for the growth and decay of ice (see the description of sea grid-points below).

Land

In the current model, all land grid-points are assumed to have constant properties, except for the occurrence of snow. No modelling of the biosphere is included. Soil temperatures and soil moisture are computed for land grid-points (see Sections 6, 7 and 8), as is snow cover. A constant roughness length z_0 = 0.168 m is used in the determination of the surface fluxes as described in Section 5. Details regarding surface albedo are given in Section 11 for radiation.

Snow

If the surface conditions are sufficiently cold, then precipitation falling on the surface is converted to snow. This snow alters the prescribed surface according to the depth of snow. The albedo of snow is reduced when the snow is melting. The maximum allowable snow depth is set at 4 m.

Sea grid-points

The sea surface has its temperature (T_s) interpolated daily from monthly data. There is no allowance for diurnal variation of sea surface temperature. Near the poles, the sea grid-points may be converted to mixed-layer ocean grid-points with self-computed temperatures, and then to ice grid-points.

Due to the presence of non-zero elevation for sea grid-points, the atmospheric temperature and moisture fields will tend to adjust to this elevation effect. The use of observed sea level (elevation = 0) temperatures will give rise to incorrect gradients between the surface and the first model level which are used in the calculation of surface fluxes. In order to correct for this, the SSTs are adjusted to account for the spectral elevations by use of a constant lapse rate of 6.5°C km^{-1}. These adjusted SSTs are then used in the calculation of sensible and latent heat flux.

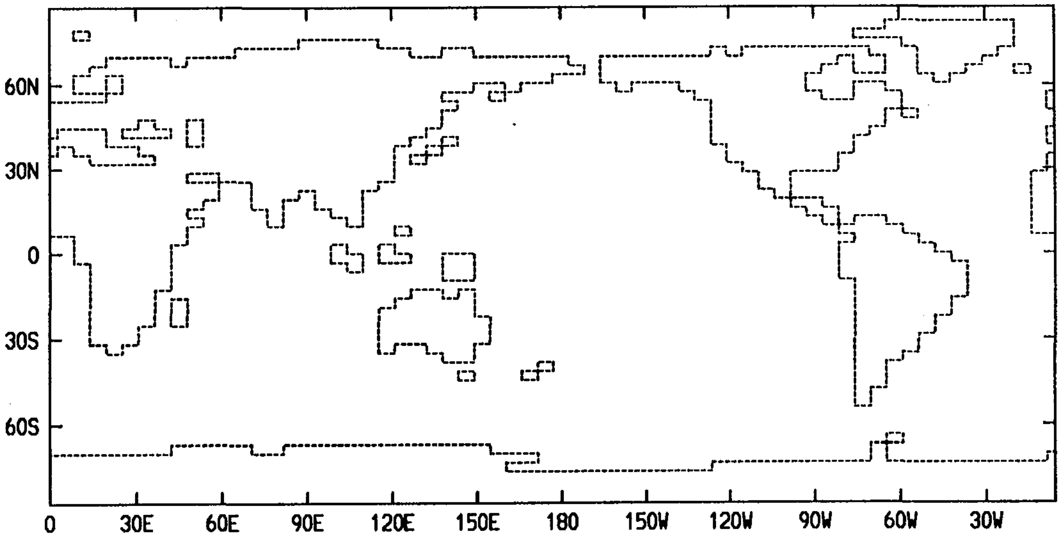

Figure 3. Outline of land masses on the R21 model grid.

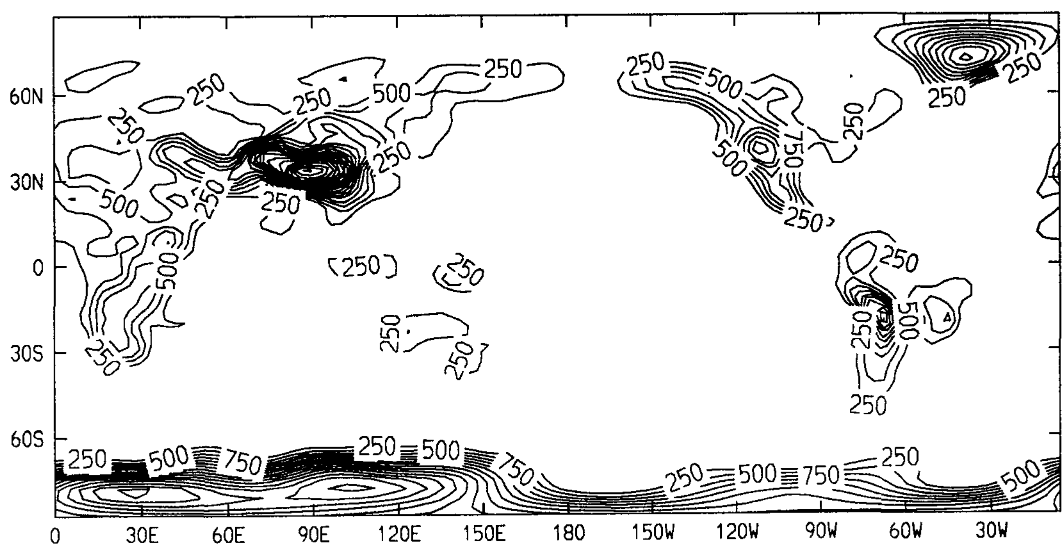

Figure 4. Topography (m) on the R21 model grid. The contour interval is 250 m.

Sea-ice grid-points

Sea-ice is formed if the temperature of the ocean (a mixed-layer point) falls below the freezing point of sea water. A simple thermodynamic ice model based largely on Parkinson and Washington (1979) is then used to allow for ice growth and decay. The sea-ice grid-points allow for snow cover, similar to land grid-points. The temperature at the air-surface interface T_s (either ice or snow) is computed as a result of the net flux of energy (from radiation, sensible heat flux, heat of sublimation and heat conduction through the ice) into the surface layer. Sublimation reduces the snow cover at grid-points with snow, and the ice amount at snow-free ice grid-points.

Heat conduction through the ice is proportional to the temperature difference between the surface and the underlying sea water (assumed to be at freezing point). There is also a prescribed flux of 2 W m^{-2} into the ice from the ocean below the ice which is included to represent the lateral convergence of heat transport by the ocean below the ice. These two fluxes are applied to heat the ice and thus, in addition to the sublimation at the surface, control the growth/decay of the ice thickness. For a description of how ice changes its horizontal extent, see the next subsection detailing the function of the mixed-layer ocean grid-points. Some constraints imposed on the sea-ice are:

i) the maximum snow depth is 4 m with the excess being compressed into ice below the snow,
ii) a maximum ice depth of 4 m is allowed.

Mixed-layer ocean grid-points

The mixed-layer ocean (MLO) grid-points act as a buffer between the sea grid-points and the ice grid-points. Note that the sea grid-points take their temperature T_s from the observed data set, whereas for ice grid-points the temperature of the sea below the sea-ice is at the freezing point of sea water (the ice/snow surface temperature is computed). For MLO grid-points, a 50 m depth is assumed and from the net energy flux at the surface the evolution of temperature for the MLO point can be obtained. However, in reality the temperature of the MLO point is not only influenced by the surface energy flux but also by the influx of heat from the surrounding sea (lateral and from below by overturning). In order that the response of the MLO grid-points be realistic (and also in part because of the diurnal forcing of the model), these effects are parameterized by a relaxation back to the observed SST for that point (with an exponential decay period of about 23 days).

As the model proceeds through an annual cycle, the MLO grid-points can reach freezing point. When this occurs, a MLO point changes to an ice point. If the equatorward point is a sea point, then this point now changes status to a MLO point. The reverse of this occurs for melting. Note that for both cases the current and the *equatorward* grid-points only change status. Since the transform loops compute a latitude at a time from each pole towards the equator the surface mask can be updated in the correct sequence.

5. Surface fluxes (*hsflux*)

If the flux into the ground is denoted by G, the net downward short-wave flux by S, the downward long-wave flux by R, the upward sensible heat flux by H_0, the upward latent heat flux by LE, then the energy balance equation linking these quantities may be written as

$$G = S + R - \sigma T_s^4 - H_0 - LE \,. \tag{5.1}$$

Here T_s represents the effective surface temperature (for long-wave radiation purposes) and σ is the Stefan-Boltzmann constant. The evaluation of S, R and T_s will be given in subsequent sections.

The surface fluxes of heat and moisture, and that of momentum are parameterized following Monin-Obukhov similarity theory. This assumes a surface layer within which the fluxes of heat and momentum are constant in the vertical. The scaling velocity u_* and temperature θ_* are defined from the heat and momentum fluxes; these are constants applying to the whole surface layer. The fluxes can be written as

$$H_0/(\rho c_p) = \overline{\theta' w'} = u_* \theta_* \tag{5.2}$$

$$|\underline{\tau}_s|/\rho = \left\{ (\overline{u'w'})^2 + (\overline{v'w'})^2 \right\}^{1/2} = u_*^2 . \tag{5.3}$$

In the Louis (1979) method these equations are rewritten as functions of the bulk Richardson number

$$Ri_b = g \frac{\partial \theta}{\partial z} / \left\{ \theta \left| \frac{\partial V}{\partial z} \right|^2 \right\} \tag{5.4}$$

$$u_*^2 = C_{DN} \; |\underline{V}| \; F_m(z/z_0 \,,\, Ri_b) \; |\underline{V}| \tag{5.5}$$

$$u_* \theta_* = C_{HN} \; |\underline{V}| \; F_h(z/z_T \,,\, Ri_b) \; (\theta_s - \theta_1) \tag{5.6}$$

where C_{DN} and C_{HN} are the neutral transfer coefficients for momentum and heat respectively corresponding to height z. In this section and also in Appendix B and Section 9, θ is a column-wise potential temperature defined to equal T_s at the surface (p_s is used rather than p_{1000}); this provides the proper units for the sensible heat flux equation (5.2) to be compatible with the soil fluxes,

$$\theta = T \left(\frac{p_s}{p} \right)^{R/c_p} . \tag{5.7}$$

Note that the separate components of the momentum flux are given by

$$\rho \overline{u'w'} = \rho \; C_{DN} \; |\underline{V}| \; F_m \; (u_s - u_1) \tag{5.8}$$

$$\rho \overline{v'w'} = \rho \; C_{DN} \; |\underline{V}| \; F_m \; (v_s - v_1) \tag{5.9}$$

where the surface velocity components u_s, v_s are taken to be zero.

The roughness lengths for heat (z_T) and momentum (z_0) are different over land, with $z_0/z_T = 7.4 \approx e^2$; this corresponds to the currently accepted value of 0.4 for